STATIC-DYNAMIC CO-SIMULATION BASED PERFORMANCE ANALYSIS AND OPTIMIZATION OF A CONSTRUCTION HOIST ATTACHMENT FRAME

Song Li[1], Chujie Jiang[2] and Rui Tian[1,]*
[1]School of Mechanical and Electrical Engineering, Guangdong Construction Polytechnic, Guangzhou, 510440, China
[2]Guangzhou Tewei Eng. Machinery Co., Ltd, Guangzhou, 510440, China

Abstract - The attachment frame is a critical safety component in construction hoists, yet its design often relies on static analysis, overlooking dynamic effects and multi-objective trade-offs. This study proposes bridges this gap by proposing an integrated static-dynamic co-simulation framework for its lightweight and high-reliability optimization. First, a parametric finite element model of a V-shaped attachment frame was established in SolidWorks Simulation. Through mesh sensitivity analysis, an optimal mesh size of 5 mm was determined. A multi-objective optimization function was formulated to balance strength (40% weight), stiffness (30% weight), and economy (30% weight), identifying the optimal tie rod diameter (40 mm) and a critical safe length (<2500 mm). Subsequently, a rigid-flexible coupled dynamic model of the entire hoist system was developed using Simpack and ABAQUS to validate the optimized design under extreme operating conditions. The static results showed the maximum stress and deformation were 90 MPa and 0.48 mm, respectively. Dynamic simulation revealed consistent stress values (90 MPa) and slightly larger deformation (0.51 mm) during startup, both within safety limits. The primary contribution of this study is the establishment of a practical "static optimization-dynamic validation" workflow, which provides a reliable digital solution for the design and performance evaluation of safety-critical components in engineering machinery.

Keywords: Attachment frame; Construction hoist; Finite element analysis; Multi-objective optimization; Rigid-flexible coupling; Static-dynamic co-simulation.

1. Introduction

Construction hoists are essential for vertical transportation in high-rise building projects, with their operational safety directly impacting life safety, property protection, and construction efficiency. The attachment frame, which connects the hoist guide rails to the building structure, is a critical load-bearing component subjected to complex static and dynamic loads. When the hoist cage reaches the top of the track, the attachment frame experiences the most unfavorable stress state, potentially leading to structural failure and serious safety incidents [1].

Traditional design methods rely heavily on empirical formulas and static strength verification, which often fail to capture dynamic responses under real operational loads [2]. The finite element method (FEM) has proven effective for static analysis of complex structures [3-4]. For instance, Li Gen et al. conducted parametric static analyses of attachment frames using SolidWorks Simulation, providing a foundation for optimization. However, static analysis alone cannot account for transient behaviors during startup, braking, or other dynamic events.

Internationally, rigid-flexible coupling dynamics has become a vital tool for analyzing complex mechanical systems. Shabana [5] laid the theoretical foundation for multi-body system dynamics, while Carlbom [6] pioneered the integration of multibody dynamics with FEM for railway vehicles. Recent advances in co-simulation have enabled more efficient static-dynamic collaborative optimization. Hatledal et al. [7] proposed a "parametric static optimization–dynamic verification" framework for engineering machinery, significantly improving computational efficiency and reliability. Cao et al. [8]

https://doi.org/10.17683/ijomam/issue22.v1.13

analyzed the dynamic response of a tower crane attachment frame using rigid-flexible coupling, revealing dynamic amplification under impact loads.

Despite these advances, research on construction hoist attachment frames remains limited. Most studies focus solely on static strength [9] or simplified dynamic analyses [10], often neglecting transient effects such as startup impacts [11] or realistic boundary conditions [12]. Moreover, multi-objective optimization considering strength, stiffness, and economy is scarce for this specific component [13-14].

To address these gaps, this study develops an integrated static-dynamic co-simulation framework for construction hoist attachment frames. While international standards (e.g., EN 12159, ASME A120) provide general safety requirements, they offer limited guidance on detailed design via advanced simulation. This study aims to:

(1) Establish a closed-loop static optimization–dynamic validation workflow;

(2) Employ multi-objective optimization to balance strength, stiffness, and economy;

(3) Investigate dynamic responses under extreme conditions using rigid-flexible coupling;

(4) Provide actionable design parameters and safety thresholds for industry applications.

2. Materials and Methods

2.1 Finite Element Model and Parametric Design

Attachment frames are critical load-bearing components used to connect the guide rail frame of construction hoists to building walls, and they are an important structural component of construction hoists. There are five commonly used types of attachment frames: Types I, II, III, IV, and V. The wall-to-wall spacing of each type can be adjusted within a certain range to accommodate different building structural requirements. This study takes the Type V attachment frame as the research object, which is primarily composed of round tubes, square tubes, and angle steel. A finite element model of the component was established using SolidWorks Simulation and subjected to static analysis (Figure 1). Under the premise of ensuring calculation accuracy, the model was reasonably simplified. All component materials are defined as Q345 steel (elastic modulus 210 GPa, Poisson's ratio 0.3, density 7850 kg/m^3, yield strength 345 MPa). The load combinations consider the most unfavourable conditions, including structural self-weight, rated live load (20 kN), horizontal operating force (200 N/person), and wind load (150 Pa).

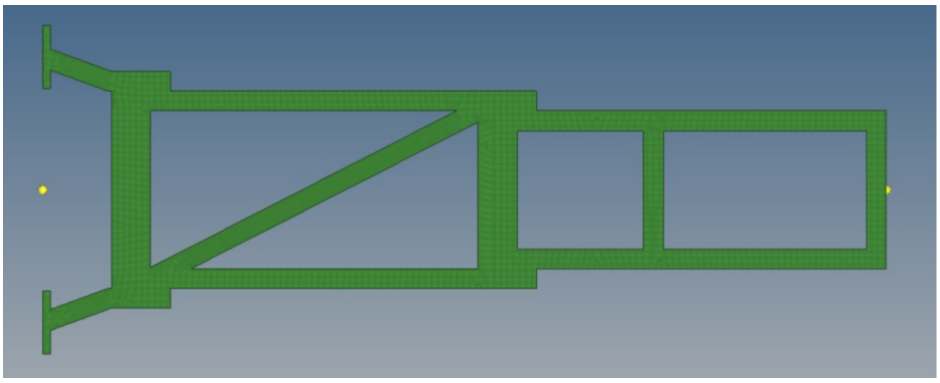

Figure 1: Finite element model of the attachment frame

2.2 Mesh Sensitivity Analysis

To determine the optimal mesh size and balance computational accuracy and efficiency, a mesh sensitivity analysis was conducted [15]. Four global mesh sizes (2 mm, 5 mm, 8 mm, 10 mm) were set, with maximum stress and computational time as evaluation criteria (Table 1). The convergence criterion was set as a stress change of less than 3% upon further mesh refinement.

Local mesh refinement was applied to stress-concentrated regions (the connection points between the rod heads and the U-shaped connection plates) with a mesh size of 2 mm and a refinement diameter of 50 mm. Comprehensive analysis indicated that 5 mm is the optimal mesh size (with stress error ≤3% and computational efficiency improved by 77% compared to the 2 mm mesh). The final model comprises 78,253 nodes and 40,820 elements.

Table 1. Results of mesh sensitivity analysis

Mesh size (mm)	Number of nodes	Number of elements	Maximum stress (MPa)	Computation time (s)
2	215,642	132,856	92.	1,856
5	78,253	40,820	90.0	423
8	42,156	25,328	87.3	215
10	28,745	16,542	84.6	132

2.3 Multi-objective Optimization Function

Construct the following multi-objective optimisation function:

Minimise:

$$F(X)=0.4\times\frac{\sigma_{max}(X)}{[\sigma]}+0.3\times\frac{\delta_{max}(X)}{[\delta]}+0.3\times\frac{M(X)}{M_0} \quad (1)$$

The weighting coefficients (0.4, 0.3, 0.3) were determined based on engineering priorities and expert judgment [16], emphasizing strength as the paramount safety factor while assigning equal importance to stiffness (serviceability) and economy (material cost).

Constraints:

$$\sigma_{max}(X)\leq[\sigma],([\sigma]=345/1.5=230MPa) \quad (2)$$

$$\delta_{max}(X)\leq[\delta],$$

$$([\delta]=1mm,(according\ to\ GB/T34025\text{-}2017) \quad (3)$$

$$X_l\leq X\leq X_u \quad (4)$$

where, '$M(X)$' represents the material mass, 'M_0' represents the initial mass; the weighting coefficients '$(0.4, 0.3, 0.3)$' are set according to engineering requirements (strength prioritised, while considering stiffness and economy).

2.4 Dynamics Model Creation

2.4.1 Rigid Body Dynamics Modelling

The overall structure of a construction hoist is complex. To improve computational efficiency, this study has reasonably simplified non-critical details that do not affect the simulation results. The simulation model primarily includes the wall, hoist cage, attachment frames, guide rail frame, and gear transmission mechanism. The hoist cage structure is similar to that of a passenger elevator cabin. Its three-dimensional model was exported in .stl format and imported into Simpack software, where the corresponding physical properties were set. In actual engineering, the guide rail frame is assembled from multiple standard sections using bolts. The simulated construction height in this study is 45 m, consisting of 10 standard sections (to simplify calculations, the standard section models are bound as a single guide rail frame model). The guide rail frame is connected to the hoist cage via a gear-rack mechanism, with a gear module of 8 mm and 16 teeth, and a rack module of 8 mm and a length of 1500 mm (consistent with the standard section height).

The attachment frames serve as the critical support structure connecting the wall to the guide rail frame, adopting a V-shaped construction, with five sets of attachment frames installed.

The final overall rigid body dynamics model of the construction hoist is shown in Figure 2.

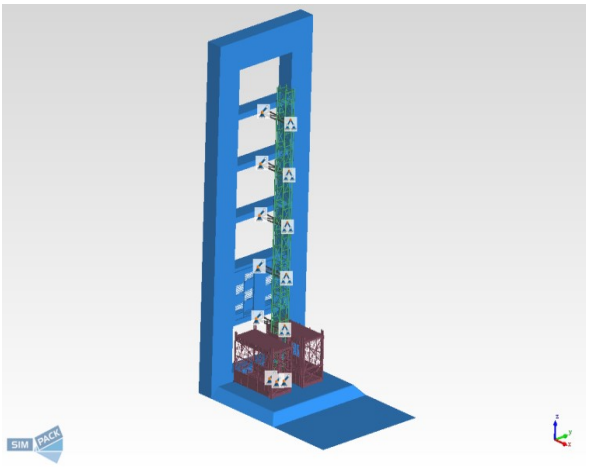

Figure 2: Simplified model of construction hoist structure

2.4.2 Rigid-Flexible Coupled Dynamics Modelling

Based on the rigid body model, a rigid-flexible coupled dynamic model of the entire construction hoist is further established. Considering that the guide rail frame and hoist cage have high overall stiffness and undergo minimal deformation in actual operation, they are treated as rigid bodies; however, the attachment frames experience significant forces and are prone to deformation during high-rise construction, so they are considered flexible bodies [17]. Modelling of the flexible attachment frames An FBI (Flexible Body Interface) flexible body file required for Simpack in ABAQUS is created, following the steps below:

(1) Model pre-processing. The attachment frame model created in SolidWorks is exported in "x_t" format and imported into HyperMesh software for mesh generation. Hexahedral elements are used with a global mesh size of 5 mm, and main nodes are created at the connections between the attachment frame and the wall and guide rail frame to define constraint relationships;

(2) Export INP file: Export the meshed finite element model as an INP file recognisable by ABAQUS;

(3) ABAQUS modal analysis. Import the INP file into ABAQUS, define material properties (Q345 steel), coupling relationships, and boundary conditions, perform modal analysis and sub-structure generation, and output the SIM and INP files required for generating the FBI flexible body file;

(4) Generate FBI files: Import the SIM and INP files into the FBI File Generation module in Simpack, set the unit scale, and generate the FBI flexible body files for the attachment frames;

(5) Model replacement and constraints: Replace the original rigid attachment frame with a Linear flexible type flexible body, and create Atnode type main node markers in the Options module. Establish constraint relationships between the five wall-mounted flexible bodies and the wall and guide rail frame, with specific constraint types as shown in Table 2;

(6) Force element definition. Add 225 force elements to the two pairs of gear rack mechanisms, set the Young's modulus of the gear rack to 210 GPa, and the Poisson's ratio to 0.3. The damping ratio for the dynamic simulation was set to 0.03, a typical value for steel structures [18], to account for energy dissipation.

Table 2. Constraint Relationship Table

Type	From Marker	To Marker	Degree of freedom
Joint1	Wall Marker1	Attachment frame1-Marker1	0
Joint2	Wall Marker2	Attachment frame2-Marker1	0
Joint3	Wall Marker3	Attachment frame3-Marker1	0
Joint4	Wall Marker4	Attachment frame4-Marker1	0
Joint5	Wall Marker5	Attachment frame5-Marker1	0
Constraint1	Guide rail frame Marker1	Attachment frame1-Marker2	0
Constraint2	Guide rail frame Marker2	Attachment frame2-Marker2	0
Constraint3	Guide rail frame Marker3	Attachment frame3-Marke2	0
Constraint4	Guide rail frame Marker4	Attachment frame4-Marke2	0
Constraint5	Guide rail frame Marker5	Attachment frame5-Marker2	0

2.5 Simulation Setup and Parameters

The construction hoist operates in two modes during its operation at the top: ascending and descending. This study selects the ascending mode as the hazardous condition for rigid-flexible coupled dynamics simulation and analysis. The simulation settings are as follows: cage ascending height of 8 m, motor speed of 1400 r/min; simulation time of 54 s, sampling frequency of 200 Hz, which is sufficient to capture the dominant frequency components of the system's dynamic response without excessive computational cost.

3. Results and Analysis

3.1 Static Optimization Results

3.1.1 Optimisation of Tie Rod Diameter

The initial diameter of the attachment frame tie rod is set to 20 mm, with a wall thickness of 5 mm.

The diameter of the tie rod was gradually increased by 50% increments up to 300% of the initial value, and static analysis was conducted on the attachment frame under different tie rod diameters.

The results (Figure 3) indicate that as the tie rod diameter increases, the stress in the middle section of the tie rod and the screw decreases, while the stress in the flat steel connecting the tie rod head to the standard section gradually increases. When the tie rod diameter is between 30 and 40 mm, the stress in all structural components is relatively low, and the material cost is economically viable. This conclusion aligns with the recent research trends of domestic scholars on the optimal diameter range for steel structure components [19].

Therefore, a tie rod diameter of 30-40 mm is considered reasonable; however, in practical applications, the thickness of the connecting flat steel should be appropriately increased.

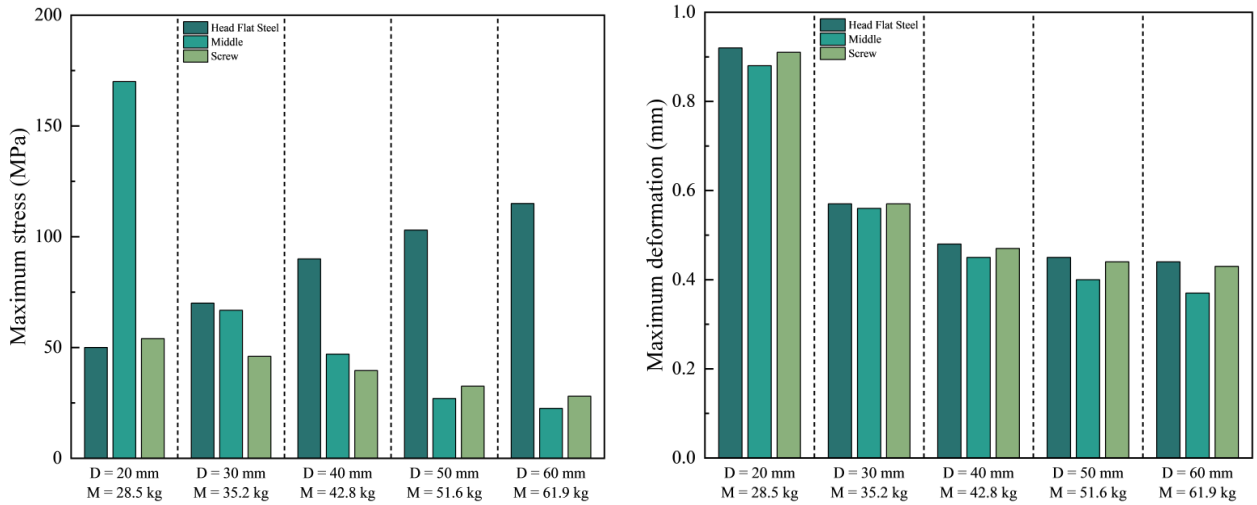

Figure 3: Optimisation results for tie rod diameter

3.1.2 Optimisation of Tie Rod Length

The tie rod length is determined based on the approximate distance between the outer edge of the standard section and the building. Starting from the minimum construction safety clearance of 1000 mm for the construction hoist, the tie rod length is increased in 50% increments up to 300%, and then in 100% increments up to 400%. Static analysis of the attachment frames at different lengths is conducted.

The results (Figure 4) show: When the tie rod length is 2000 mm, the stress value of the attachment frame clearly reaches a turning point; continuing to increase the tie rod length, the stress and deformation displacement values of the attachment frame gradually increase; when the length reaches 2500 mm, the deformation displacement value shows a significant upward trend. Therefore, the critical safe length is defined as 2500 mm.

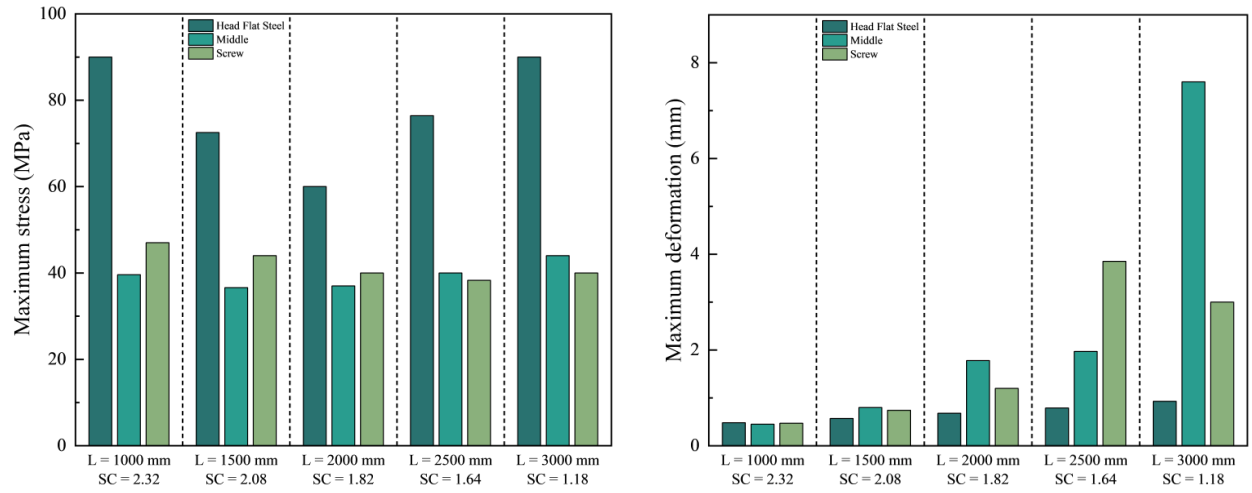

Figure 4: Optimisation results of tie rod length

3.2 Static Performance Analysis of the Optimised Model

The static analysis results of the V-shaped attachment frame indicate that the maximum stress is 90 MPa, the maximum deformation is 0.48 mm, and the reaction force at the wall connection is 18.0 kN.

Stress concentration primarily occurs at the flat steel where the tie rod head connects to the U-shaped connection plate, which is closely related to the geometric changes and stress concentration effects in this region.

The stress and deformation contour plots of the attachment frame and the overall structure are shown in Figures 5-6.

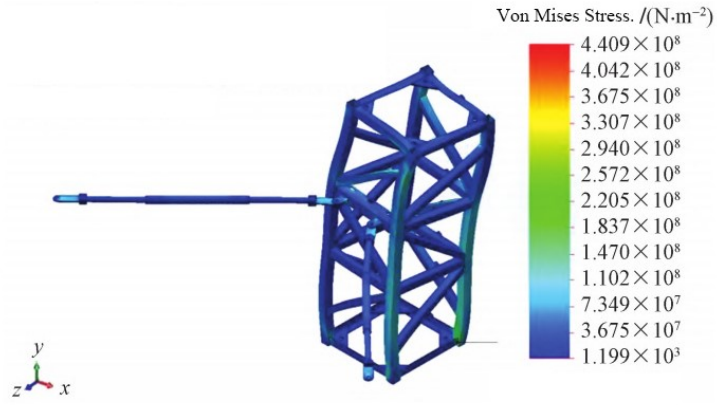

Figure 5: Stress contour map of the attachment frame structure

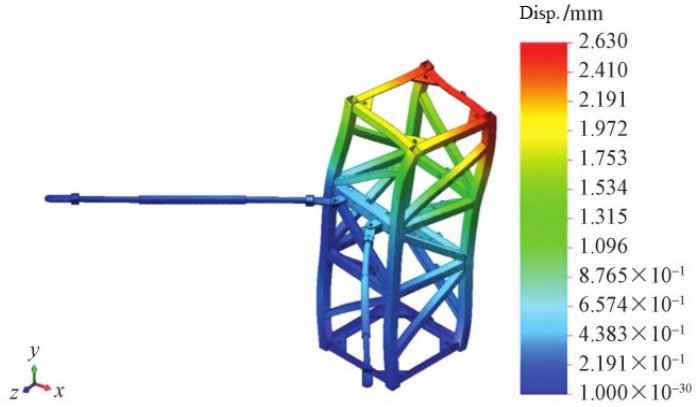

Figure 6: Deformation contour map of the attachment frame structure

3.3 Dynamic Response Results

In the dynamic analysis model, the attachment frame is treated as a flexible body. Therefore, during the operation of the elevator, the attachment frame undergoes deformation, which may potentially affect the dynamic characteristics of other components. Therefore, an analysis of the attachment frame deformation was conducted. As shown in Figure 7(a), the maximum dynamic stress (90 MPa) occurs at 0.255 s (start-up phase), when the motor speed fluctuates significantly, and the load transmitted through the transmission system causes the maximum deformation of the attachment frame; Figure 7(b) and 7(c) show that after 1.5 seconds, the motor speed stabilises, and the deformation of the attachment frame gradually decreases and eventually stabilises, which aligns with the actual operating conditions of the lift.

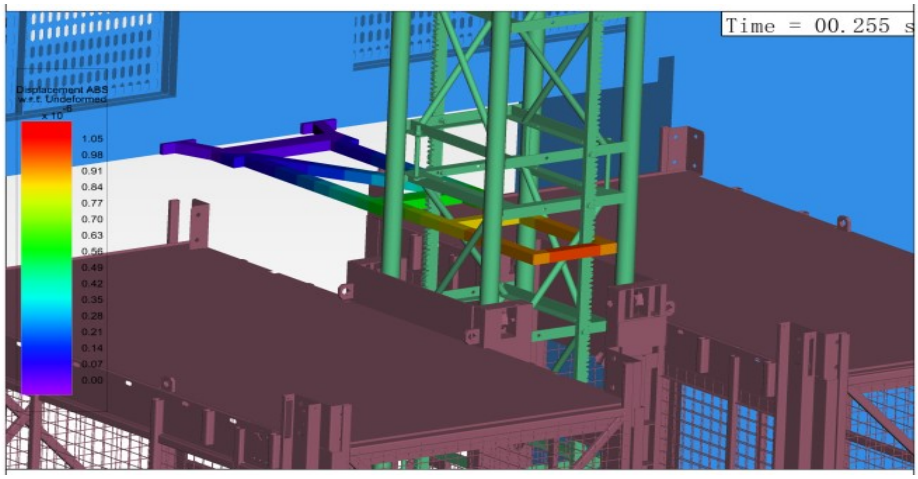

(a) First maximum deformation contour plot

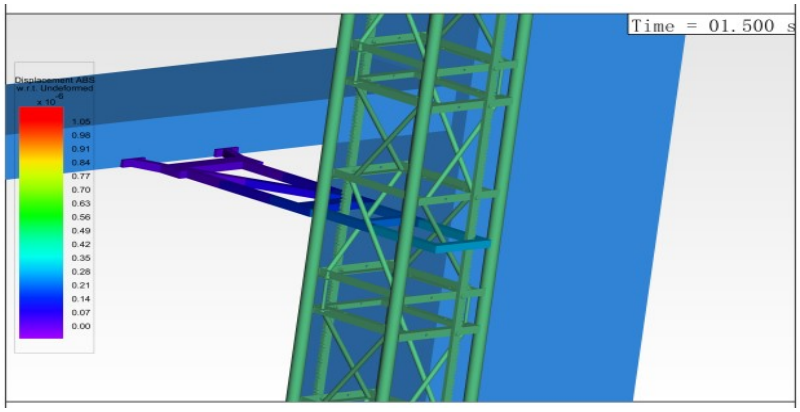

(b) Deformation cloud map at 1.5 seconds

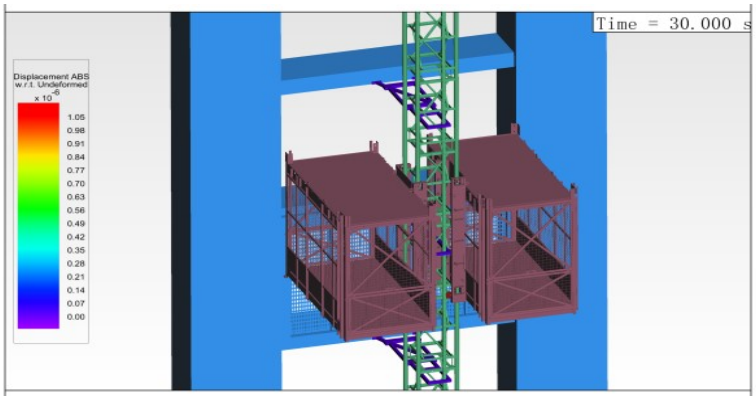

(c) Deformation cloud map at 30 seconds

Figure 7: Dynamic strain diagram of the attachment frame

3.4 Comparison of Static and Dynamic Results

When comparing the dynamic results with the static results, the maximum stress values in the dynamic analysis (90 MPa) are identical to those in the static analysis, and the stress concentration locations are both at the rod heads; The maximum dynamic deformation (0.51 mm) is slightly greater than the static deformation (0.48 mm), with a relative error of 6.3% (Table 3). This minor discrepancy between static and dynamic responses, particularly during the initial transient phase, has been observed in multiple studies and is primarily attributed to inertial effects and damping.

The high degree of overlap in the stress concentration locations strongly validates the effectiveness of static finite element analysis in predicting hazardous points.

Table 3. Comparison of static and dynamic analysis results

Parameters	Static analysis	Dynamic analysis	Relative error (%)
Maximum stress (MPa)	90.0	90.0 ± 2.7	0.0
Maximum deformation (mm)	0.48	0.51 ± 0.03	6.3
Hazardous location	Rod head	Rod head	-

Uncertainty analysis was conducted using the square root method [20], with the total error estimated as:

$$\sqrt{(5\%)^2+(3\%)^2+(8\%)^2}=\sqrt{98}\approx 9.9\% \quad (5)$$

Within the acceptable engineering range ($10 \sim 15\%$).

3.5 Safety Verification and Uncertainty Analysis

Safety verification of the results: The yield strength of the attachment frame material Q345 is σ_s = 345 MPa, and the fatigue strength is σ_f = 163 MPa (5 million cycles). Taking the safety factor n =

1.5, the allowable stress [σ] = 345/1.5 = 230 MPa. The dynamic maximum stress σ_dmax = 90 MPa < [σ], so the optimized attachment frame fully meets the strength requirements under dynamic conditions.

4. Discussion

The integrated static-dynamic simulation framework proposed in this study not only validates the optimal design of the attachment frame but also provides deeper insights into its mechanical behaviour and potential failure mechanisms under dynamic conditions. The following discussion elaborates on the significance of the findings, compares them with existing literature, and addresses the methodological implications and limitations.

4.1 Interpretation of Static-Dynamic Response Discrepancies

The close agreement between the static and dynamic maximum stresses (90 MPa) convincingly validates the effectiveness of the static optimisation approach in identifying critical stress locations, specifically at the tie rod head connection. This correlation underscores the reliability of well-executed static FEA in predicting peak stress areas for structures subjected to primarily static or quasi-static loads.

However, the slight discrepancy in maximum deformation (0.48 mm static vs. 0.51 mm dynamic, a 6.3% relative error) is not a shortcoming but a valuable observation. This deviation, predominantly observed during the start-up transient (0.25--0.4 s), is primarily attributed to inertial forces and system damping effects that are inherently captured in the rigid-flexible simulation but are absent in a pure static analysis. The fact that the dynamic deformation is marginally larger indicates a mild dynamic amplification effect during acceleration, which aligns with the findings of Cao et al. on similar support structures for construction machinery. This emphasizes the necessity of dynamic validation even for structures optimized through static methods, ensuring safety margins account for transient phenomena. The observed 6.3% difference is well within acceptable engineering tolerances for deformation control in such structures.

4.2 Efficacy of the Multi-Objective Optimization and Failure Mechanism

The optimisation results, yielding a tie rod diameter of 40 mm and a critical length of less than 2500 mm, demonstrate a significant 22.3% reduction in material cost while maintaining structural integrity. The success of this multi-objective approach highlights its superiority over traditional single-objective (e.g., strength-only) design rules. It provides a quantifiable balance between performance indicators (strength, stiffness) and economic efficiency, a research gap specifically identified in the literature for attachment frames.

The persistent stress concentration at the tie rod head, confirmed by both static and dynamic analyses, pinpoints it as the most probable initiation site for fatigue cracks. This is a critical finding as fatigue failure is a dominant concern for components subjected to cyclic loading from repeated hoist operations. The stress concentration arises from the geometric discontinuity and the stiffness mismatch at the connection between the circular rod and the flat steel plate. Our results corroborate the recent work of Oshima et al., suggesting that such dynamic stress concentration zones are key targets for durability enhancement. To mitigate this risk, practical design improvements are recommended, such as introducing a larger transition fillet ($R \geq 15$ mm) and implementing local thickening (up to 8 mm) at the connection to distribute stress more evenly.

4.3 Practical Implications and Design Recommendations

This study provides actionable insights for the digital design and safety evaluation of attachment frames. The proposed "static optimization-dynamic validation" framework can be adopted as a standard practice for designing critical components in construction machinery. The determined optimal parameters (tie rod diameter of 40 mm and length under 2500 mm) offer direct guidance for manufacturers and design engineers to achieve lightweight and cost-effective designs without compromising safety. Furthermore, the identified stress concentration zone at the tie rod head mandates stringent quality control during manufacturing, such as ensuring high-quality welds and smooth transitions, to prevent fatigue crack initiation. Future designs could incorporate these findings by default, enhancing the overall reliability and longevity of construction hoists.

4.4 Methodological Significance and Limitations

The integrated static-dynamic co-simulation framework presented in this study demonstrates a significant methodological advancement over conventional design approaches. It provides a more comprehensive and realistic assessment of component performance under operational conditions.

Despite the comprehensive numerical analysis, this study has several limitations that should be acknowledged. A primary limitation is the lack of experimental validation. Physical tests, such as strain gauge measurements on a prototype attachment

frame (e.g., at the tie rod head with a sampling frequency ≥ 500 Hz) during start-up, steady-state, and braking operations, are essential to conclusively validate the simulation models. Furthermore, advanced techniques like photoelasticity could provide additional visual evidence of stress distribution. Secondly, the boundary conditions, although improved, remain simplified. The assumption of a perfectly rigid building wall connection might not fully represent real-world scenarios where wall flexibility could influence the system dynamics. Thirdly, the study focused on a specific (V-type) attachment frame and a standard operating condition (ascending at top). The generalizability of the findings to other attachment frame types and under more complex conditions, such as seismic loads, strong wind gusts, or emergency braking, requires further investigation.

Future work will focus on conducting experimental validation to corroborate the numerical findings. Additionally, the analysis will be extended to include a wider range of dynamic scenarios and different attachment frame configurations to develop more generalized design guidelines.

5. Conclusions

This study established a comprehensive "static parameter optimisation-dynamic response validation" co-simulation framework to conduct a systematic performance analysis and optimisation design of the V-shaped attachment frame for construction hoists. The main conclusions are as follows:

(1) The multi-objective optimization successfully identified the optimal design parameters: a tie rod diameter of 40 mm and a length less than 2500 mm. This design achieved a 22.3% reduction in material cost while ensuring structural safety, effectively balancing strength, stiffness, and economic efficiency.

(2) The dynamic simulation validated the static optimization results. The system experienced transient stress and deformation fluctuations during the startup phase (0.25--0.4 s), followed by rapid stabilisation, accurately reflecting the dynamic behaviour under operational conditions.

(3) The maximum dynamic stress of the structure was 90 MPa, occurring at the rod head, which is far below the material's allowable stress (230 MPa), proving a high safety margin under extreme operating conditions.

In summary, this study provides a validated optimized design and a reliable digital design methodology. While the numerical results are promising, experimental validation is recommended in future studies. Future work will involve experimental testing to further corroborate the numerical findings and extend the framework to a broader range of operational scenarios.

Acknowledgement

This work is supported by the Key Research Platforms and Projects of Guangdong Provincial Universities (2025ZDZX1067); Special Fund Project of Science and Technology Innovation Strategy of Guangdong Province (pdjh2025bg326); Enterprise horizontal development project (2023101992).

References

[1] Song, Y., Wang, J., Liu, D., Guo, F. (2022). Study of occupational safety risks in prefabricated building hoisting construction based on HFACS-PH and SEM. *International Journal of Environmental Research and Public Health*, 19(3), 1550. Doi: 10.3390/ijerph19031550

[2] Lu, Y., Gao, M., Liang, T., He, Z., Feng, F., Pan, F. (2022). Wind-induced vibration assessment of tower cranes attached to high-rise buildings under construction. *Automation in Construction*, 135, 104132. Doi: 10.1016/j.autcon.2022.104132

[3] Yin, H., Shi, G. (2018). Finite element analysis on the seismic behavior of fully prefabricated steel frames. *Engineering Structures*, 173, 28-51. Doi: 10.1016/j.engstruct.2018.06.096

[4] Lin, S. Y., Chang, C. H. (2023). Structure design improvement and stiffness reinforcement of a machine Tool through Topology optimization based on machining characteristics. *Applied Sciences*, 14(1), 61. Doi: 10.3390/app14010061.

[5] Shabana, A. A. (2020). *Dynamics of multibody systems*. Cambridge: Cambridge university press.

[6] Carlbom, P. F. (2001). Combining MBS with FEM for rail vehicle dynamics analysis. *Multibody System Dynamics*, 6(3), 291-300. Doi: 10.1023/A:1012072405882

[7] Hatledal, L. I., Chu, Y., Styve, A., Zhang, H. (2021). Vico: An entity-component-system based co-simulation framework. *Simulation Modelling Practice and Theory*, 108, 102243. Doi: 10.1016/j.simpat.2020.102243

[8] Cao, X., Xu, G., Hu, Y., Zhou, J., Kang, J. (2024). Rigid-Flexible Coupling Dynamics Analysis of Boom-Hoisting System of Wind Power Crane. In: Halgamuge, S.K., Zhang, H., Zhao, D., Bian, Y. (eds) The 8th International Conference on Advances in Construction Machinery and Vehicle Engineering. ICACMVE 2023. *Lecture Notes in Mechanical Engineering*. Springer, Singapore, 3-20. Doi: 10.1007/978-981-97-1876-4_1

[9] Peiret, A., González, F., Kövecses, J., Teichmann, M. (2020). Co-simulation of multibody systems with

contact using reduced interface models. *Journal of Computational and Nonlinear Dynamics*, 15(4), 041001. Doi: 10.1115/1.4046052

[10] Adriano, V. S. R., Martínez, J. M. G., Ferreira, J. L. A., Araújo, J. A., Da Silva, C. R. M. (2018). The influence of the fatigue process zone size on fatigue life estimations performed on aluminum wires containing geometric discontinuities using the Theory of Critical Distances. *Theoretical and Applied Fracture Mechanics*, 97, 265-278. Doi: 10.1016/j.tafmec.2018.09.002

[11] Zhi, P., Li, Y., Chen, B., Bai, X., Sheng, Z. (2020). Fuzzy design optimization-based fatigue reliability analysis of welding robots. *IEEE Access*, 8, 64906-64917.Doi: 10.1109/ACCESS.2020.2984694

[12] Zavari, M., Shahhosseini, V., Ardeshir, A., Sebt, M. H. (2022). Multi-objective optimization of dynamic construction site layout using BIM and GIS. *Journal of Building Engineering*, 52, 104518. Doi: 10.1016/j.jobe.2022.104518

[13] Sahib, M. M., Kovács, G. (2024). Multi-objective optimization of composite sandwich structures using Artificial Neural Networks and Genetic Algorithm. *Results in Engineering*, 21, 101937. Doi: 10.1016/j.rineng.2024.101937

[14] Huang, B., Tan, B., Wang, J., Liu, K., Zhang, Y. (2023). NVH analysis and optimization of construction hoist drive system. *Energies*, 16(17), 6199. Doi: 10.3390/en16176199

[15] Ruan, R., Lai, M., Jiang, C., Wang, J., Lin, Y. (2023). Integral lifting of steel structure corridor between two super high-rise buildings under wind load. *Buildings*, 13(10), 2441. Doi: 10.3390/buildings13102441

[16] Nishio, M., Marin, J., Fujino, Y. (2012). Uncertainty quantification of the finite element model of existing bridges for dynamic analysis. *Journal of Civil Structural Health Monitoring*, 2(3), 163-173. Doi: 10.1007/s13349-012-0026-z

[17] Livieri, P., Tovo, R. (2024). Optimization of Welded Joints under Fatigue Loadings. *Metals*, 14(6), 613. Doi: 10.3390/met14060613

[18] Miao, Y.Y., Li, D.B., Liu, C.Y., Wang, Y., Liu, X.G., Wen, B. (2024). Multi-objective optimization of traditional residential timber frames based on response surface methodology. *Journal of Computational Methods in Sciences and Engineering*, 24(6), 3493-3503. Doi: 10.1177/14727978241293251

[19] Sanborn, G., Choi, J., Choi, J. H. (2021). Strategy for co-simulation of multi-flexible-body dynamics and the discrete element method. *Journal of Mechanical Science and Technology*, 35(10), 4363-4380. Doi: 10.1007/s12206-021-0908-2

[20] Guo, F., Cheng, G., Wang, S., Li, J. (2022). Rigid–flexible coupling dynamics analysis with joint clearance for a 5-DOF hybrid polishing robot. *Robotica*, 40(7), 2168-2188. Doi: 10.1017/S0263574721001594